American Mineralogist, Volume 97, pages 856–863, 2012

The genesis of mantle-derived sapphirine

Ben-Xun Su,[1,*] Hong-Fu Zhang,[1,*] Yan Hu,[1] M. Santosh,[2] Yan-Jie Tang,[1] and Yan Xiao[1]

[1]State Key Laboratory of Lithospheric Evolution, Institute of Geology and Geophysics, Chinese Academy of Sciences, P.O. Box 9825, Beijing 100029, China
[2]Department of Interdisciplinary Science, Kochi University, Akebono-cho 2-5-1, Kochi 780-8520, Japan

Abstract

Sapphirine, a typical ultrahigh-temperature metamorphic mineral, is rarely found in mantle xenoliths. Here we report the occurrence and characteristics of sapphirine in a mantle-derived xenolith from the Cenozoic basalts of Hannuoba in the North China Craton. The xenolith consists of a clinopyroxene, spinel, and sapphirine assemblage, with the sapphirine occurring as the reaction rim surrounding spinel. The mineral compositions of this sample are all characterized by high Mg contents, similar to those of minerals from other sapphirine-bearing rocks reported from high-Mg-Al granulites elsewhere in the world. Clinopyroxene is relatively rich in Al and Ca in comparison to pyroxene in peridotite and pyroxenite xenoliths in the Hannuoba basalts, as well as in global mafic and felsic granulites in other terranes, a feature that is consistent with the bulk composition. The *P-T* compilations from both experimental and natural rock data show a restricted stability field for the coexisting clinopyroxene + spinel + sapphirine assemblage of around 8–15 kbar and 800–900 °C. The rare occurrence of sapphirine in a mantle-derived xenolith therefore suggests specific bulk composition, restricted *P-T* range and possible melt-peridotite interaction. Such conditions are best satisfied in a tectonic setting with basaltic magma underplating and interaction between the infiltrating melts and the wall-rock peridotite.

Keywords: Sapphirine, pyroxenite, *P-T* condition, North China Craton

Introduction

Experimental studies and *P-T* estimates from natural assemblages and mineral phase equilibria modeling have constrained the stability of sapphirine under ultrahigh-temperature (UHT) and medium- to high-pressure conditions of 900–1100 °C and 10–18 kbar, corresponding to lower crustal and upper mantle depths (e.g., Ackermand et al. 1975; Sills et al. 1983; Powell and Holland 1985; Griffin and O'Reilly 1986; Christy 1989; Das et al. 2006; Sato et al. 2006; Brigida et al. 2007; Podlesskii et al. 2008; Kelsey 2008). Sapphirine has been reported in Mg-Al granulites subjected to extreme crustal metamorphism under UHT conditions in various regions of the world (e.g., Lal et al. 1987; Okay 1994; Santosh et al. 2007, 2009; Galli et al. 2011; Jiao and Guo 2011). The stability of sapphirine-bearing assemblages in metamorphic orogens exhumed from depth has been a topic of wide interest in characterizing metamorphic *P-T* conditions, tectonic architecture, and crustal evolution (e.g., Sills et al. 1983; Christy 1989; Okay 1994; Mattielli et al. 1996; Gregoire et al. 2001; Harley 2004; Santosh et al. 2007, 2009, 2012; Tsunogae and Santosh 2011; Tsunogae et al. 2011; Xiang et al. 2012).

Mantle-derived sapphirine has been rarely reported, such as in pyroxenite xenoliths from Stockdale, Kansas (Meyer and Brookins 1976), from Delegate, New South Wales, Australia (Griffin and O'Reilly 1986), the Beni Bousera massif, Morocco (Kornprobst et al. 1990), and the Ronda massif, Spain (Morishita et al. 2001). Sapphirine in these pyroxenites exhibits diverse textural relationships despite the relatively consistent mineral assemblages, suggesting that sapphirine occurs in a wide range of *P-T* conditions and bulk compositions. Griffin and O'Reilly (1986) suggested that sapphirine is stable under upper-mantle conditions in Ca-Al-Mg-rich bulk compositions, whereas Okay (1994) suggested that the vast majority of sapphirine-bearing rocks are rich in Mg and Al and poor in Ca, consistent with the composition of the mineral. Sapphirine occurs as relics of a low-*P* mafic granulite assemblage preserved in garnet in Okay's (1994) study. Christy (1989) suggested that sapphirine might be a widespread constituent of basic rocks with high Mg/(Mg+Fe) ratio. The models proposed to explain the origin of sapphirine in such rocks include recycling of crustal material (Morishita et al. 2001) and exsolution of clinopyroxene (Kornprobst et al. 1990; Mattielli et al. 1996).

The Cenozoic Hannuoba basalts occur along the northern part of the Trans-North China Orogen, a Paleoproterozoic suture that amalgamates the Western and Eastern Blocks in the North China Craton. Abundant lower crustal and upper mantle xenoliths are found in the basalts and have been studied by various workers (Fan et al. 2001; Liu et al. 2010; Rudnick et al. 2004; Zhang 2009; Zheng et al. 2009; Zhang et al. 2011, 2012). However, the present study is the first report of sapphirine-bearing rocks from Hannuoba. We present detailed petrologic and geochemical data on the sapphirine-bearing clinopyroxenite from Hannuoba and compare our results with other occurrences in an attempt to characterize the origin of mantle-derived sapphirine, as well as suggest possible chemical discriminants between sapphirines of crustal and mantle origins.

* E-mail: subenxun@mail.igcas.ac.cn; hfzhang@mail.igcas.ac.cn

0003-004X/12/0506–856$05.00/DOI: http://dx.doi.org/10.2138/am.2012.3859

Geological background and sample descriptions

The Tertiary Hannuoba basalt field is located on the northern margin of the North China Craton (Fig. 1a) and has been dated at 22 to 14 Ma (Liu et al. 1990). It is best known for its abundance of diverse mantle and crustal xenoliths. The mantle-derived xenoliths vary in composition from peridotite (dunite, harzburgite, lherzolite, and wehrlite) to garnet- and spinel-facies pyroxenite (e.g., Chen et al. 2001; Xu 2002; Zhou et al. 2002; Rudnick et al. 2004; Liu et al. 2005; Tang et al. 2007; Zhang et al. 2012), whereas the crustal xenoliths are basically divided into mafic and felsic types (e.g., Fan et al. 2005; Liu et al. 2005; Zheng et al. 2009; Jiang and Guo 2010). These xenoliths are mainly found in three localities: Damaping, Zhouba, and Jieshaba (Fig. 1b).

The sapphirine-bearing clinopyroxenite (JSB10-57) studied here was collected from Jieshaba. The gray-green xenolith within host basalt shows rounded edges and measures approximately 25 × 15 × 5 cm and has a medium-grained equigranular texture. There are only three kinds of rock-forming minerals in this sample, namely clinopyroxene (~90% by mode), spinel (9%), and sapphirine (1%). The clinopyroxene is sub-rounded and 1–3 mm in length (Fig. 2a). Some grains show well-developed cleavage along which orthopyroxene exsolution lamellae occur in some grains (Figs. 2b, 2c, and 2d). Some grain boundaries and fractures show a locally spongy-texture enclosing tiny ilmenite and glass (Figs. 2c and 2e). Spinel is optically light green, subhedral to anhedral in form, and occurs either as inclusions in, or as discrete grains between adjacent clinopyroxenes (Figs. 2b and 2d). Two types of spinel are identified: a fine-grained (<0.3 mm) variety and a second type (>0.2 mm) rimmed by sapphirine (Figs. 2b–2f). Sapphirine occurs as thin, pale-blue rims (<150 µm) grown around spinel grains. Sapphirine is also found as symplectitic intergrowths with secondary spinel or clinopyroxene; occasionally inclusions of clinopyroxene are trapped within the sapphirine (Fig. 2e), with a rim of secondary spinel surrounding the enclosed sapphirine (Fig. 2f).

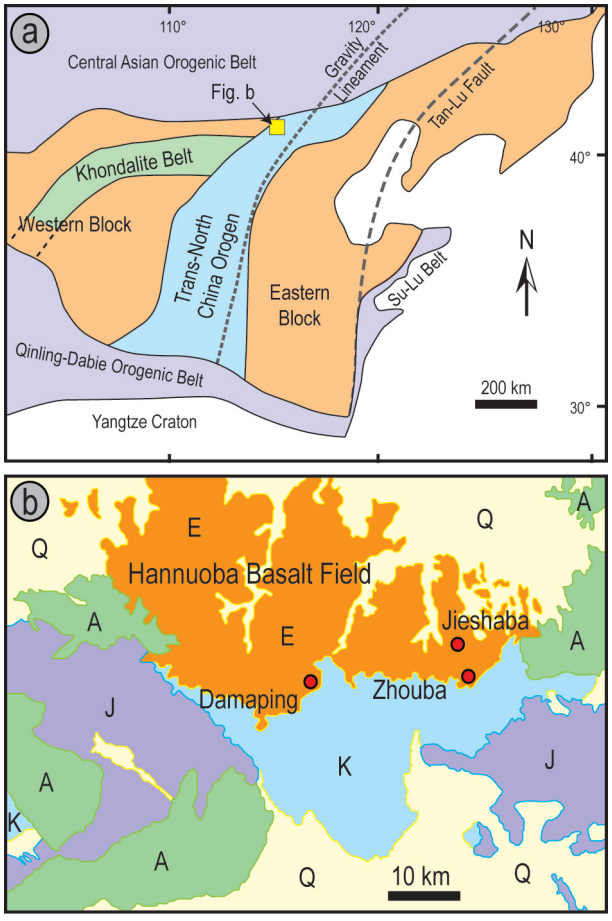

Figure 1. (**a**) Map showing the location of the Hannuoba basalt filed in the northern North China Craton. (**b**) Sample locality at Jiashaba in the basalt field (**b**) (modified after Zhou et al. 2002). A = Archean; J = Jurassic; K = Cretaceous; Q = Quaternary; E = Tertiary. (Color online.)

Bulk-rock chemistry and mineral composition

The bulk major element chemistry was obtained by X-ray fluorescence spectrometry (XRF) on fused glass disks using a Shimadzu XRF-1500 instrument. FeO content was analyzed by a chemical titration method and Fe_2O_3 was then recalculated using total Fe and FeO. Mineral chemistries were measured by wavelength-dispersive spectrometry (WDS) using a JEOL JXA8100 electron probe operating at an accelerating voltage of 15 kV with 12 nA beam current, 5 µm beam spot, and 10–30 s counting time. Both measurements were carried out at the Institute of Geology and Geophysics, Chinese Academy of Sciences.

The sapphirine-bearing spinel clinopyroxenite is poor in SiO_2 (40.3 wt%) and rich in Al_2O_3 (20.4 wt%). It has a remarkably high Mg no. [Mg no. = 100 × Mg/(Mg+Fe_{total})] of 85.3 with FeO/Fe_2O_3 ratio <1. The CaO content is 16.2 wt% (Table 1).

The clinopyroxenes in this sample are aluminous diopside (Al_2O_3: 5.74–10.4 wt%) with low Cr_2O_3 contents (0.12–0.16 wt%). The clinopyroxene in the spongy rim shows higher SiO_2, MgO, CaO, and apparently lower Al_2O_3 and Na_2O contents than those of the cores (Table 2). The clinopyroxene grain enclosed in sapphirine shows lower FeO content (2.80 wt%) and higher Mg no. (90.0) relative to the discrete clinopyroxene grains. Clinopyroxene has variable Fe^{2+}/Fe^{3+} ratio, and one grain analyzed shows a low Fe^{2+}/Fe^{3+} ratio of <1 (Table 2). The orthopyroxene lamellae in clinopyroxene are rich in Al_2O_3 (7.29 wt%) but poor in SiO_2 (52.4 wt%) and low in Mg no. (87.7).

The spinel in the xenolith is magnesian and aluminous (MgO: 20.4–21.4 wt%; Al_2O_3: 64.9–66.8 wt%) with low Cr_2O_3 (0.76–1.03 wt%) and TiO_2 (<0.06 wt%) and moderate FeO content (9.86–12.1 wt%) with Mg no. = 75.2–79.6. The Fe^{3+} content of spinel is remarkably lower than Fe^{2+} (Table 2). Most spinel grains, including those with sapphirine rims, are compositionally homogeneous, but some show Al depletion and Fe enrichment in the rims relative to the cores (Table 2).

Two sapphirine grains show nearly identical concentrations of SiO_2 (14.2–14.5 wt%), Cr_2O_3 (0.41–0.49 wt%), Al_2O_3 (60.1–62.3 wt%), MgO (18.8–19.5 wt%,) FeO (3.93–4.01 wt%), MnO (0.03–0.04 wt%), CaO (0.04–0.06 wt%), and Na_2O (0.01–0.07 wt%) contents with Mg no. of 89.6–89.8 (Table 2).

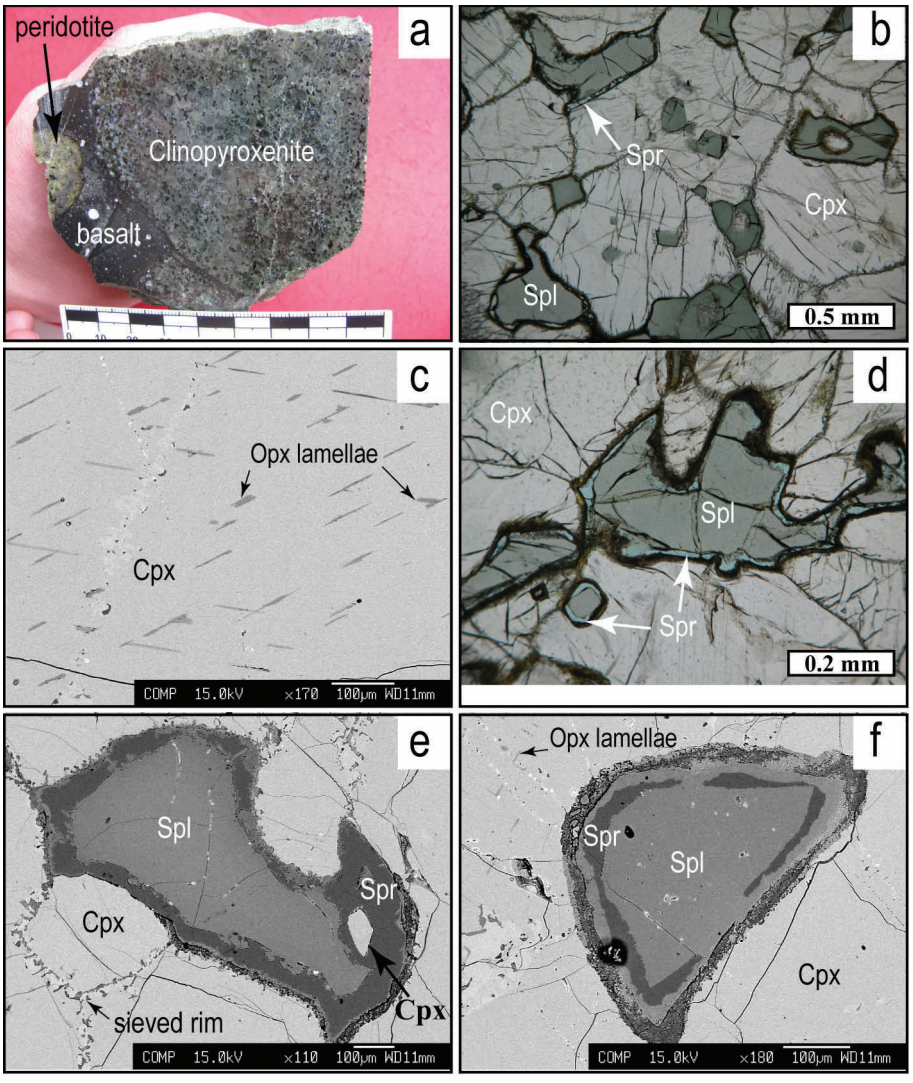

FIGURE 2. Photographs of the Hannuoba clinopyroxenite. (**a**) Hand specimen of clinopyroxenite associated with a peridotite xenolith showing a curved boundary with the host basalts. (**b**) The contact relationship between constituent minerals. Light-green spinels (Spl) occur as inclusions in clinopyroxene (Cpx), or as discrete grains mantled by sapphirine (Spr). (**c**) Backscattered electron image showing orthopyroxene (Opx) exsolution lamellae in Cpx. (**d**) Occurrence of sapphirine as prisms surrounding spinel grain. (**e**) Clinopyroxenes with spongy rims. Sapphirine occurs as rims on spinel and encloses fine-grained clinopyroxene. (**f**) Sapphirine-rimming spinel is surrounded by secondary spinel. (Color online.)

DISCUSSION

Occurrence and comparison with examples elsewhere in the world

Sapphirine-bearing metamorphic rocks generally have quite complex mineral assemblages and textural relationships. In garnet-sillimanite granulites ("khondalites"), sapphirine occurs in association with quartz in the matrix, as inclusions in garnet or sillimanite, or surrounded by matrix plagioclase (e.g., Santosh et al. 2007, 2009, 2012; Guo et al. 2008; Jiao and Guo 2011; Tsunogae and Santosh 2011), and less often, as small prisms enclosing spinel grains in their cores (e.g., Lal et al. 1987). In mafic granulites, sapphirine occurs with clinopyroxene, orthopyroxene, plagioclase, spinel, and garnet as major minerals. The sapphirine may form poikiloblasts, sometimes euhedral, or occur as coronae or symplectites (Arima and Barnett 1984; Christy 1989; Gregoire et al. 2001). Mutual exsolution and intergrowth of sapphirine and clinopyroxene has also been observed (Christy 1989; Lal 1997; Sutherland et al. 2003).

Among ultramafic bulk compositions, sapphirine has been observed only in pyroxenites with relatively simple mineralogy compared to their occurrence in mafic and felsic rocks. The host pyroxenites from orogenic massifs usually contain clinopyroxene, orthopyroxene, spinel, garnet, hornblende, phlogopite, corundum, and plagioclase (Kornprobst et al. 1990; Okay 1994; Morishita et al. 2001). The mineral assemblage of the sapphirine-bearing pyroxenite xenoliths reported by Meyer and Brookins (1976) and Griffin and O'Reilly (1986) consists of orthopyroxene, clinopyroxene, spinel, garnet, and plagioclase. In most cases, sapphirine is associated with, and may replace, spinel (Meyer and Brookins 1976; Griffin and O'Reilly 1986; Kornprobst et al. 1990). However, the Hannuoba clinopyroxenite reported here has a simpler mineral assemblage that consists of clinopyroxene-spinel-sapphirine; all sapphirines occur as rims on spinel (Figs. 2b–2f). The mineralogical constitution and microstructural features of the Hannuoba xenolith suggest that the sapphirine in this rock is genetically related to spinel, and formed either during the cooling/uplift process or through the reaction of spinel with a clinopyroxene solid solution.

TABLE 1. Bulk composition of the sapphirine-bearing clinopyroxenite xenolith (JSB10-57) from Hannuoba

SiO_2	TiO_2	Al_2O_3	TFe_2O_3	MnO	MgO	CaO	Na_2O	K_2O	P_2O_5	LOI	Total	FeO	Fe_2O_3	Mg no.
40.3	0.11	20.43	5.21	0.10	15.2	16.2	0.93	0.13	0.02	0.76	99.3	1.91	3.11	85.3

TABLE 2. Chemical composition of minerals in the sapphirine-bearing clinopyroxenite xenolith (JSB10-57) from Hannuoba

Mineral	Spl		Spr	Spl		Spr	Spl			Cpx			Cpx			Cpx	Opx lamella
Position	core	mantle	Spl rim	core	mantle	Spl rim	core	mantle	rim	core	mantle	rim	core	mantle	rim	in Spr	in Cpx
SiO_2	0.00	0.03	14.4	0.00	0.00	14.2	0.03	0.00	0.00	49.7	49.7	51.0	49.8	50.0	50.9	50.6	52.4
TiO_2	0.06	0.04	0.02	0.00	0.03	0.03	0.00	0.03	0.00	0.13	0.14	0.12	0.13	0.14	0.16	0.15	0.02
Al_2O_3	66.5	66.0	62.3	66.2	66.8	60.1	66.5	66.0	64.9	9.86	10.4	5.94	10.1	9.76	5.74	8.67	7.29
Cr_2O_3	0.99	1.03	0.49	0.94	0.98	0.41	0.83	0.79	0.76	0.13	0.11	0.08	0.15	0.13	0.10	0.10	0.04
FeO	10.7	10.4	4.01	10.7	9.86	3.93	11.0	11.3	12.1	3.04	3.02	3.11	3.04	3.00	3.03	2.80	7.78
MnO	0.11	0.06	0.04	0.12	0.04	0.03	0.08	0.17	0.23	0.10	0.09	0.11	0.13	0.10	0.07	0.02	0.15
MgO	21.2	20.9	19.5	21.4	21.4	18.8	21.3	20.6	20.4	13.2	13.1	15.1	13.1	13.2	15.6	14.0	30.9
CaO	0.01	0.03	0.04	0.04	0.02	0.06	0.01	0.00	0.03	20.8	20.8	22.8	21.2	21.3	23.0	21.6	0.51
Na_2O	0.02	0.02	0.01	0.02	0.00	0.07	0.00	0.02	0.00	1.65	1.54	0.60	1.68	1.55	0.49	1.30	0.05
K_2O	0.00	0.01	0.01	0.02	0.00	0.01	0.00	0.00	0.00	0.00	0.00	0.00	0.01	0.01	0.01	0.01	0.00
NiO	0.22	0.24	0.08	0.21	0.14	0.07	0.24	0.19	0.16	0.00	0.04	0.00	0.00	0.09	0.00	0.03	0.00
Total	99.8	98.8	100.9	99.6	99.3	97.7	99.9	99.1	98.6	98.5	98.9	98.9	99.3	99.3	99.0	99.3	99.2
O =	4	4	20	4	4	20	4	4	4	6	6	6	6	6	6	6	6
Si	0.000	0.001	1.669	0.000	0.000	1.700	0.001	0.000	0.000	1.819	1.814	1.871	1.811	1.821	1.861	1.843	1.834
Ti	0.001	0.001	0.002	0.000	0.000	0.003	0.000	0.001	0.000	0.004	0.004	0.003	0.004	0.004	0.004	0.004	0.001
Al	1.958	1.964	8.509	1.952	1.972	8.478	1.954	1.964	1.946	0.425	0.448	0.257	0.433	0.419	0.248	0.372	0.300
Cr	0.020	0.021	0.045	0.019	0.019	0.039	0.016	0.016	0.015	0.004	0.003	0.002	0.004	0.004	0.003	0.003	0.001
Fe^{3+}	0.022	0.014	0.108	0.031	0.007	0.096	0.028	0.020	0.038	0.043	0.022	0.035	0.053	0.038	0.054	0.024	0.034
Fe^{2+}	0.223	0.219	0.280	0.223	0.206	0.297	0.229	0.238	0.257	0.050	0.070	0.060	0.040	0.054	0.039	0.062	0.194
Mn	0.002	0.001	0.004	0.003	0.001	0.003	0.002	0.004	0.005	0.003	0.003	0.003	0.004	0.003	0.002	0.000	0.005
Mg	0.791	0.787	3.367	0.798	0.797	3.352	0.793	0.773	0.772	0.719	0.712	0.827	0.709	0.716	0.853	0.758	1.610
Ca	0.000	0.001	0.005	0.001	0.000	0.008	0.000	0.000	0.001	0.816	0.814	0.898	0.824	0.830	0.900	0.842	0.019
Na	0.001	0.001	0.002	0.001	0.000	0.016	0.000	0.001	0.000	0.117	0.109	0.042	0.119	0.109	0.035	0.091	0.003
K	0.000	0.000	0.001	0.001	0.000	0.002	0.000	0.000	0.000	0.000	0.000	0.000	0.000	0.000	0.001	0.000	0.000
Ni	0.005	0.005	0.007	0.004	0.003	0.007	0.005	0.004	0.003	0.000	0.001	0.000	0.000	0.003	0.000	0.001	0.000
Total	3.022	3.014	14.000	3.031	3.007	14.000	3.028	3.020	3.038	4.000	4.000	4.000	4.000	4.000	4.000	4.000	4.000

Both sapphirine and its coexisting minerals of different origins (crustal- and mantle-derived) show distinct variations in chemical composition. For example, the sapphirine in felsic granulites (khondalites) generally contain higher SiO_2 and Al_2O_3 but lower MgO and Cr_2O_3 contents, whereas those in mafic granulites display large compositional ranges in Al_2O_3 (62–71 wt%), MgO (16–21 wt%), and Cr_2O_3 (0–0.5 wt%) contents (Figs. 3a–3c). Second, coexisting clinopyroxenes in mafic granulites are diopsides with high ferrosilite (Fs) end-member (>15), low Al_2O_3 (<10 wt%) and Na_2O (<7 wt%) contents, and large Mg no. variation (70–90) (Figs. 3d–3f). Third, spinels in both felsic and mafic granulites are low in Mg no., show a wide compositional range, and are relatively poor in Al_2O_3 (Fig. 3g). In contrast, the sapphirine grains in pyroxenite xenoliths have lower Al_2O_3 (<68 wt%) but higher MgO (19–21 wt%) and Cr_2O_3 (>0.1 wt%), and their SiO_2 contents are also higher at a given Al_2O_3 level (Figs. 3a–3c). The clinopyroxenes in the pyroxenites show low Fs (<15) and high wollastonite (Wo) end-members (Fig. 3e). Their Al_2O_3 and Na_2O contents vary widely, whereas their higher Mg nos. are restricted to a relatively narrow range (Figs. 3e and 3f) indicating their mantle origin. The clinopyroxenes in the spongy rims of this study have extremely low Al_2O_3 and Na_2O contents that probably resulted from incipient melting (e.g., Griffin and O'Reilly 1986; Su et al. 2011). Finally, spinels in the pyroxenites are apparently rich in MgO and Al_2O_3 (Fig. 3g).

In summary, crustal-derived sapphirine-bearing rocks usually possess complex mineral assemblages and occurrences and display large compositional variations, consistent with their metamorphic origin during multi-stage processes at crustal depths (Powell and Holland 1988; Christy 1989; Mattielli et al. 1996; Santosh et al. 2009, 2012). On the other hand, sapphirine-bearing mantle-derived pyroxenites show relatively simple mineral assemblages and are characterized by high-Mg minerals with variable Al_2O_3 contents.

Genesis of mantle-derived sapphirine

***P-T* conditions.** The relatively simple mineralogy (Spr-Cpx-Spl; all mineral abbreviations are in the caption of Fig. 4) and the absence of appropriate mineral assemblages suitable for thermobarometry in the Hannuoba clinopyroxenite do not allow any precise *P-T* estimates for the Hannuoba clinopyroxenite. Christy's (1989) compilation from experimentally determined and calculated results define the *P-T* conditions for Spr-Cpx associations as 9–14 kbar and 800–900 °C (Fig. 4a; see references in Christy 1989). The continuous univariant spinel-sapphirine transition extends from 1 kbar, around 650 °C through 10 kbar, 770 °C (Seifert 1974) to the invariant point at 22 kbar, 880 °C (Ackermand et al. 1975), which is constrained by the reaction of Clin + Crn + Spl = Spr + H_2O (Fig. 4a; Okay 1994). Gasparik's study on the reaction of Grt = Spl + Opx + An ± Cpx ± Spr revealed that sapphirine could be stable at 9–10 kbar over the temperature range of 700–1000 °C (Gasparik 1984). Taking into account the reaction of Grt + Fo = Cpx + Opx + Spl, a gray line-filled *P-T* field bound by 8–15 kbar and 800–900 °C is obtained for the coexisting Cpx + Spl + Spr assemblage in the present study (Fig. 4a). This field is divided into two parts by the spinel to garnet pyroxenite transition established by Herzberg (1978) at ca.10 kbar. The lower part is the stability field for sapphirine in

garnet pyroxenite, and the upper part is the field for sapphirine-bearing spinel pyroxenite. This is in good agreement with *P-T* estimates for natural rocks such as: 10–14 kbar, 800–1000 °C from the Stockdale locality (Meyer and Brookins 1976); 14 kbar, 1005 °C for Delegate (Griffin and O'Reilly 1986); and ca. 10 kbar, 800–900 °C for Ronda (Morishita et al. 2001).

Previous studies on the Hannuoba pyroxenites yielded temperatures in the range of 850–1000 °C estimated by mineral pair thermometry (e.g., Chen et al. 2001; Liu et al. 2003; Zheng et al. 2009). The spinel pyroxenite occurs at 30–40 km depths, which is regarded as the crust-mantle transition zone, and garnet pyroxenite is located below at 40–60 km depths (Fig. 4b; Chen et al. 2001; Fan et al. 2005). We thus infer that the sapphirine-bearing spinel clinopyroxenite from Hannuoba formed at about 10 kbar, 850–900 °C.

Petrologic and geochemical constraints. Pyroxenites cover a variety of rocks ranging from orthopyroxenites, through websterites, to clinopyroxenites, and are generally considered to have formed under high pressure in melts flowing along conduits in the mantle (e.g., Downes 2007). However, in recent years, a metasomatic origin by means of peridotite-melt interaction has received wide attention (Garrido and Bodinier 1999; Liu et al. 2005; Sobolev et al. 2005; Zhang 2009; Zhang et al. 2010). Liu et al. (2005) and Tang et al. (2011) ascribed the formation of Hannuoba pyroxenite to peridotite-melt interaction based on petrological and geochemical characteristics. In terms of mineral chemistry, clinopyroxenes in the pyroxenites display high Mg no. and large variations in some major oxides, such as SiO_2, Al_2O_3, and CaO, resembling those in peridotite (Figs. 5a–5c). Similar features are also observed in spinels (Fig. 5d).

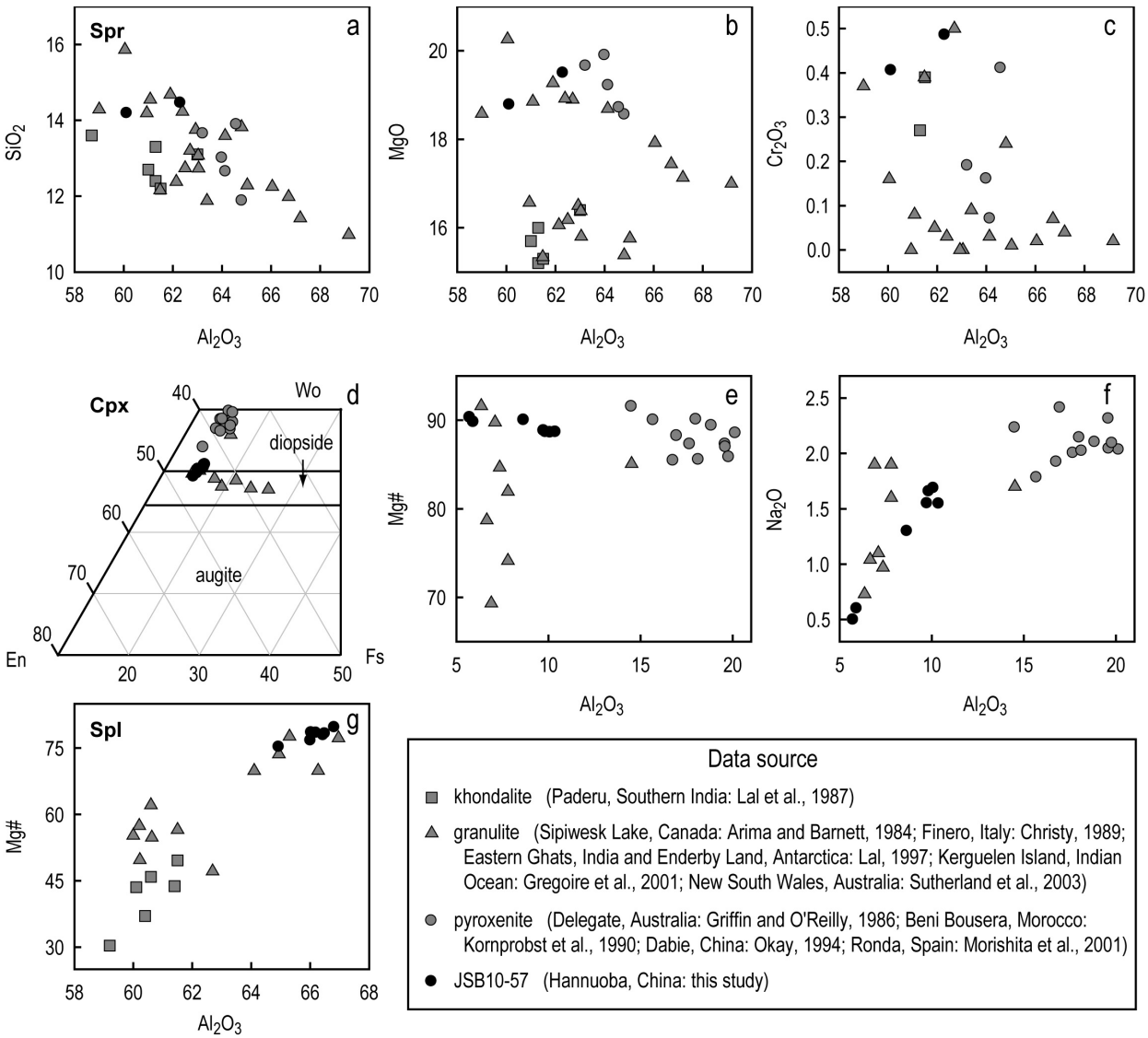

FIGURE 3. A comparison of the compositions of sapphirine, clinopyroxene, and spinel from different settings including khondalite, granulite, and pyroxenite. See text for details.

Furthermore, sample JSB10-57 shows distinct bulk SiO_2/Al_2O_3 ratio relative to the Hannuoba sapphirine-free pyroxenites and host basalts (Fig. 5e; Zheng et al. 2009 and references therein), and its low Fe^{2+}/Fe^{3+} character in the bulk-rock composition is mainly controlled by spinel composition. Therefore, we consider that the pyroxenites from Hannuoba are probably genetically linked to the peridotites through reaction with an Al-Ca-Mg-rich melt. Alternatively, the oxygen ratio of sapphirine lies between those of spinel and pyroxene, and may be produced by a sliding reaction: $2MgAl_2O_4$ (Spl) + 2"$Mg_{0.75}Al_{2.5}Si_{0.75}O_6$" (in pyroxene) = $Mg_{3.5}Al_9Si_{1.5}O_{20}$ (Spr). The unrealistic, highly aluminous pyroxene composition can be rewritten: $2MgAl_2O_4$ (Spl) + $2.5MgAlSiO_6$ (in Cpx or Opx) = $Mg_{3.5}Al_9Si_{1.5}O_{20}$ (Spr) + $0.5Mg_2Si_2O_6$ (in Cpx or Opx) (Christy 1989). Thus, sapphirine grows at the expense of spinel, and clinopyroxene loses Mg and Al, becoming closer to diopside in composition.

The occurrences of sapphirine in pyroxenites, including both this study and those in previous reports from elsewhere, indicate that the Spr-Cpx-Spl association developed from spinel clinopyroxenite. The available mineral-phase equilibra reactions cannot adequately explain this association without the involvement of a melt phase. This further confirms that an interaction between peridotite and melt must have taken place during pyroxenite formation. The xenolith might have undergone extensive subsolidus re-equilibration as indicated by the presence of exsolution lamellae, coronas, and intergrowth textures (Fig. 2; Mattielli et al. 1996; Gregoire et al. 2001). Furthermore, despite the abundant occurrence of garnet pyroxenites and spinel pyroxenites in the Hannuoba basalts, sapphirine-bearing rocks have not been reported until now. Therefore, only under unusual conditions can sapphirine develop in mantle depths, i.e., restricted *P-T*, specific bulk composition, and appropriate interaction with mantle peridotites. These features possibly explain why sapphirine is rarely found in mantle-derived rocks.

Geological significance

The defined *P-T* conditions (Fig. 4a) indicate that the mantle depths where the sapphirine equilibrated are typically characterized by elevated geothermal gradients and juvenile materials (Ackermand et al. 1975; Mattielli et al. 1996). This is in accordance with the presence of pyroxenites (with or without sapphirine) in the crust-mantle transition zone beneath the Hannuoba area (Fig. 4b) where the geothermal gradient is computed to be much higher than the oceanic geotherm (Chen et al. 2001; Su et al. 2007). The 10 km thick transitional zone located at about 30 to 40 km beneath the Hannuoba area (Fig. 4b) is best explained by varying degrees of mixing through voluminous basaltic magmas into the mantle wall-rock. In addition, the intermediate-mafic granulite xenoliths entrained by Hannuoba basalts carrying abundant Mesozoic zircons are noted to be compositionally high in Mg no. (e.g., Zheng et al. 2009; Jiang and Guo 2010; Liu et al. 2010). These observations agree with the magma underplating model (e.g., Zhou et al. 2002; Fan et al. 2005; Liu et al. 2005; Zheng et al. 2009; Zhang et al. 2012); in addition to providing the heat input, the magmas might also have contributed to the compositional modifications required to equilibrate sapphirine in these rocks.

The high Mg, Al, and Ca contents of sapphirine-bearing mantle rocks have been evaluated in various studies. Morishita et al. (2001) suggested that such compositional characteristics result mainly from the incorporation of recycled crust. However, Gregoire et al. (1994, 1998) explained the occurrence of sapphirine

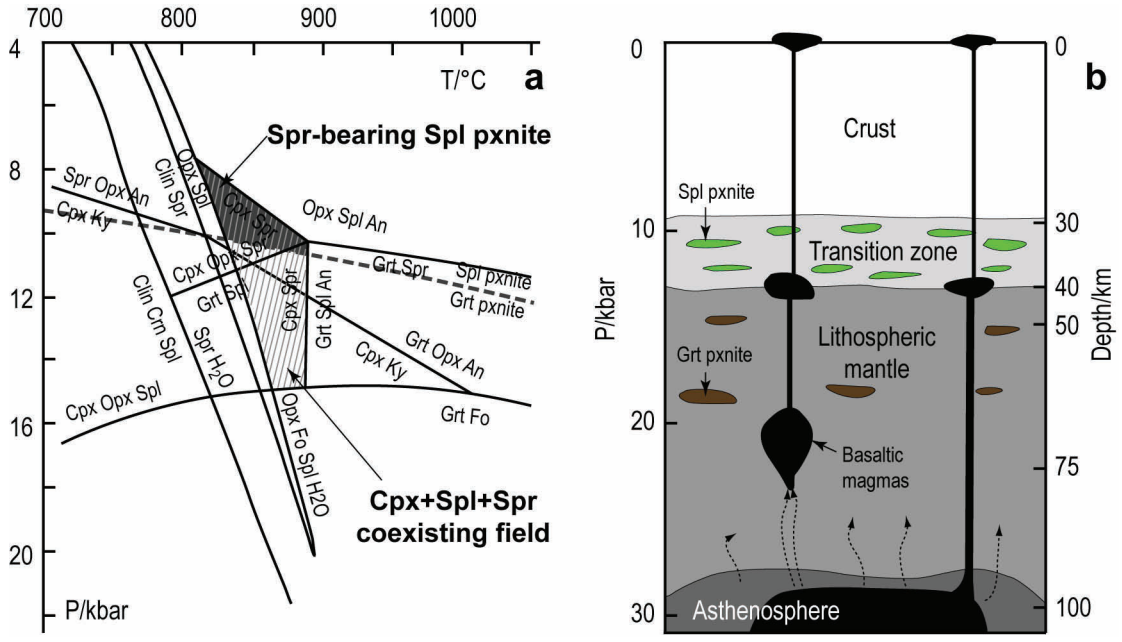

FIGURE 4. (**a**) *P-T* diagram showing the equilibrium curves of sapphirine-related reactions compiled from Ackermand et al. (1975), Herzberg (1978), Christy (1989, and references therein), and Okay (1994). (**b**) Schematic diagram showing the distribution of rock-types and inferred lithospheric mantle structure beneath Hannuoba (modified from Chen et al. 2001). Spr = sapphirine; Spl = spinel; pxnite = pyroxenite; Opx = orthopyroxene; An = plagioclase; Clin = clinochlorite; Ky = kyanite; Grt = garnet; Crn = corundum; Fo = forsterite. (Color online.)

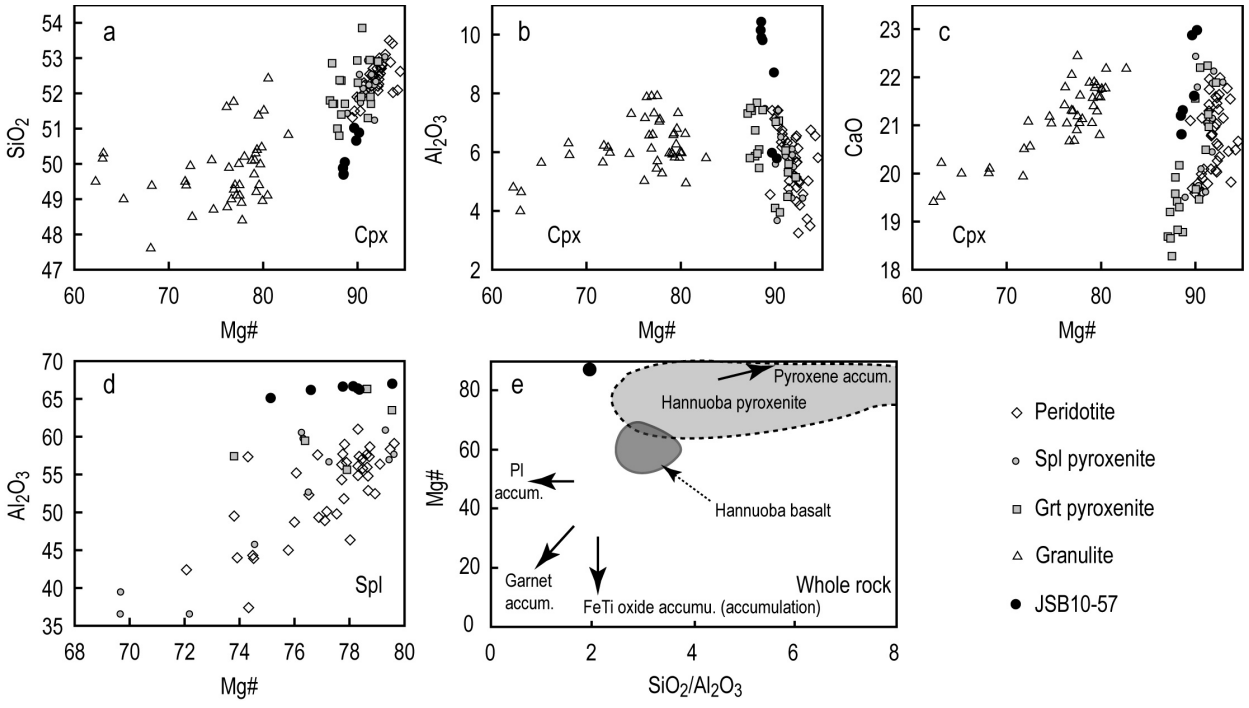

Figure 5. (**a**–**c**) Comparison of the compositions of clinopyroxene from the Hannuoba peridotite, spinel pyroxenite, garnet pyroxenite, granulite, and sapphirine-bearing spinel clinopyroxenite (JSB10-57). Data are compiled from Chen et al. (2001), Liu et al. (2003), Rudnick et al. (2004), Fan et al. (2005), and Tang et al. (2007). (**d**) Comparison of the compositions of spinel from the Hannuoba peridotite, spinel pyroxenite, garnet pyroxenite, and sapphirine-bearing spinel clinopyroxenite (JSB10-57). Data are compiled from Chen et al. (2001), Rudnick et al. (2004), and Tang et al. (2007). (**e**) Mg no. vs. SiO_2/Al_2O_3 diagram for Hannuoba pyroxenite xenoliths. The fields of Hannuoba pyroxenite and basalt are from Zheng et al. (2009, and references therein). Note that Mg no. is defined as $Mg/(Mg+0.85Fe_{total})$, to be consistent with Kempton and Harmon (1992). Unbroken arrows show the generalized direction of compositional change with accumulation of the mineral phase indicated.

from oceanic components and Ackermand et al. (1975) inferred that water also plays a major role in producing the sapphirine (Fig. 4a). Subducted oceanic crust has also been proposed as the source of parental magmas for pyroxenites to account for their compositional diversity (Medaris et al. 1995; Xu 2002; Liu et al. 2010; Yu et al. 2010; Zhang et al. 2010).

Acknowledgments

This work was financially supported by the National Science Foundation of China (Grants 40973012, 91014007, 41173011, and 41003016) and the China Postdoctoral Science Foundation to Ben-Xun Su. The authors appreciate the careful comments and constructive reviews from Stefano Poli and another anonymous reviewer and the editorial handling by Matthias Gottschalk.

References cited

Ackermand, D., Seifert, F., and Schreyer, W. (1975) Instability of sapphirine at high pressures. Contributions to Mineralogy and Petrology, 50, 79–92.

Arima, M. and Barnett, R.L. (1984) Sapphirine bearing granulites from the Sipiwesk Lake area of the late Archean Pikwitonei granulite terrain, Manitoba, Canada. Contributions to Mineralogy and Petrology, 88, 102–112.

Brigida, C., Poli, S., and Valle, M. (2007) High-temperature phase relations and topological constraints in the quaternary system $MgO-Al_2O_3-SiO_2-Cr_2O_3$: An experimental study. American Mineralogist, 92, 735–747.

Chen, S.H., O'Reilly, S.Y., Zhou, X.H., Griffin, W.L., Zhang, G.H., Sun, M., Feng, J.L., and Zhang, M. (2001) Thermal and petrological structure of the lithosphere beneath Hannuoba, Sino-Korean Craton, China: evidence from xenoliths. Lithos, 56, 267–301.

Christy, A.G. (1989) The stability of sapphirine + clinopyroxene: implications for phase relations in the $CaO-MgO-Al_2O_3-SiO_2$ system under deep-crustal and upper mantle conditions. Contributions to Mineralogy and Petrology, 102, 422–428.

Das, K., Fujino, K., Tomioka, N., and Miura, H. (2006) Experimental data on Fe and Mg partitioning between coexisting sapphirine and spinel: an empirical geothermometer and its application. European Journal of Mineralogy, 18, 49–58.

Downes, H. (2007) Origin and significance of spinel and garnet pyroxenites in the shallow lithospheric mantle: ultramafic massifs in orogenic belts in Western Europe and NW Africa. Lithos, 99, 1–24.

Fan, Q.C., Sui, J.L., Liu, R.X., and Zhou, X.M. (2001) Eclogite facies garnet-pyroxenite xenolith in Hannuoba area: New evidence of magma underplating. Acta Petrologica Sinica, 17, 1–6 (in Chinese with English abstract).

Fan, Q.C., Zhang, H.F., Sui, J.L., Zhai, M.G., Sun, Q., and Li, N. (2005) Magma underplating and Hannuoba present crust-mantle transitional zone composition: xenolith petrological and geochemical evidence. Science in China (D), 48, 1089–1105.

Galli, A., Le Rayon, B., Schmidt, M.W., Burg, J.P., Caddick, M.J., and Reusser, E. (2011) Granulites and charnockites of the Gruf Complex: Evidence for Permian ultra-high temperature metamorphism in the Central Alps. Lithos, 124, 17–45.

Garrido, C.J. and Bodinier, J.L. (1999) Diversity of mafic rocks in the Ronda peridotite: evidence for pervasive melt-rock reaction during heating of subcontinental lithosphere by upwelling asthenosphere. Journal of Petrology, 40, 729–754.

Gasparik, T. (1984) Experimentally determined stability of clinopyroxene + garnet + corundum in the system $CaO-MgO-Al_2O_3-SiO_2$. American Mineralogist, 69, 1025–1035.

Gregoire, M., Mattielli, N., Nicollet, C., Cottin, J.Y., Leyrit, H., Weis, D., Shimizu, N., and Giret, A. (1994) Oceanic mafic granulite from the Kerguelen Archipelago. Nature, 367, 360–363.

Gregoire, M., Cottin, J.Y., Giret, A., Mattielli, N., and Weis, D. (1998) The meta-igneous granulite xenoliths from Keruguelen Archipelago: evidence of a continent nucleation in an oceanic setting. Contributions to Mineralogy and Petrology, 133, 259–283.

Gregoire, M., Jackson, I., O'Reilly, S.Y., and Cottin, J.Y. (2001) The lithospheric mantle beneath the Kerguelen Islands (Indian Ocean): petrological and petrophysical characteristics of mantle mafic rock types and correlation with seismic profiles. Contributions to Mineralogy and Petrology, 142, 244–259.

Griffin, W.L. and O'Reilly, S.Y. (1986) Mantle-derived sapphirine. Mineralogical

Magazine, 50, 635–640.
Guo, J.H., Chen, Y., Peng, P., Windley, B., and Sun, M. (2008) Highly silica-undersaturated sapphirine granulites from the Daqingshan area, Western Block, North China Craton: Paleoproterozoic UHT metamorphism. In W.J. Xiao, M.G. Zhai, X.H. Li, and F. Liu, Eds., Proceedings of International Conference on Gondwana Correlation and Connection, Gondwana 13 in China (Dali), 64–65.
Harley, S.L. (2004) Extending our understanding of ultrahigh-temperature crustal metamorphism. Journal of Mineralogical and Petrological Sciences, 99, 140–158.
Herzberg, C. (1978) Pyroxene geothermometry and geobarometry: experimental and thermodynamic evaluation of some subsolidus phase relations involving clinopyroxenes in the system CaO-MgO-Al_2O_3-SiO_2. Geochimica et Cosmochimica Acta, 42, 945–957.
Jiang, N. and Guo, J.H. (2010) Hannuoba intermediate-mafic granulite xenoliths revisited: assessment of a Mesozoic underplating model. Earth and Planetary Science Letters, 293, 277–288.
Jiao, S.J. and Guo, J.H. (2011) Application of the two-feldspar geothermometer to ultrahigh-temperature (UHT) rocks in the khondalite belt, North China craton and its implications. American Mineralogist, 96, 250–260.
Kelsey, D.E. (2008) On ultrahigh-temperature crustal metamorphism. Gondwana Research, 13, 1–29.
Kempton, P.D. and Harmon, R.S. (1992) Oxygen isotope evidence for large-scale hybridization of the lower crust during magmatic underplating. Geochimica et Cosmochimica Acta, 56, 971–986.
Kornprobst, J., Piboule, M., Roden, M., and Tabit, A. (1990) Corundum-bearing garnet clinopyroxenites at Beni Bousera (Morocco): original plagioclase-rich gabbros recrystallized at depth within the mantle? Journal of Petrology, 31, 717–745.
Lal, R.K. (1997) Internally consistent calibrations for geothermobarometry of high-grade Mg-Al rich rocks in the system MgO-Al_2O_3-SiO_2 and their application to sapphirine-spinel granulites of Eastern Ghats, India and Enderby Land, Antarctica. Proceedings of the Indian Academy of Sciences, 106, 91–113.
Lal, R.K., Ackermand, D., and Upadhyay, H. (1987) *P-T*-X relationship deduced from corona textures in sapphirine-spinel-quartz assemblages from Paderu, Southern India. Journal of Petrology, 28, 1139–1168.
Liu, R., Chen, W., Sun, J., and Li, D. (1990) K-Ar age and tectonic environment of Cenozoic volcanic rock in China. In R. Liu, Ed., Age and Geochemistry of Cenozoic Volcanic Rock in China. p. 1–43. Seismology Published House, Beijing (in Chinese).
Liu, Y.S., Gao, S., Liu, X.M., Chen, X.M., Zhang, W.L., and Wang, X.C. (2003) Thermodynamic evolution of lithosphere of the North China craton: records from lower crust and upper mantle xenoliths from Hannuoba. Chinese Science Bulletin, 48, 2371–2377.
Liu, Y.S., Gao, S., Lee, C.T.A., Hu, S.Y., Liu, X.M., and Yuan, H.L. (2005) Melt-peridotite interactions: links between garnet pyroxenite and high-Mg no. signature of continental crust. Earth and Planetary Science Letters, 234, 39–57.
Liu, Y.S., Gao, S., Hu, Z.C., Gao, C.G., Zong, K.Q., and Wang, D.B. (2010) Continental and oceanic crust recycling-induced melt-peridotite interactions in the Trans-North China Orogen: U-Pb Dating, Hf isotopes and trace elements in zircons from mantle xenoliths. Journal of Petrology, 51, 537–571.
Mattielli, N., Weis, D., Gregoire, M., Mennessier, J.P., Cottin, J.Y., and Giret, A. (1996) Kerguelen basic and ultrabasic xenoliths: evidence for long-lived Kerguelen hotspot activity. Lithos, 37, 261–280.
Medaris, L.G., Beard, B.L., Johnson, C.M., Valley, J.W., Spicuzza, M.J., Jelinek, E., and Misar, Z. (1995) Garnet pyroxenite and eclogite in the Bohemian Massif: geochemical evidence for Variscan recycling of subducted lithosphere. Geologische Rundschau, 84, 489–505.
Meyer, H.O.A. and Brookins, D.G. (1976) Sapphirine, sillimanite, and garnet in granulite xenoliths from Stockdale kimberlite, Kansas. American Mineralogist, 61, 1194–1202.
Morishita, T., Arai, S., and Gervilla, F. (2001) High-pressure aluminous mafic rocks from the Ronda peridotite massif, southern Spain: significance of sapphirine- and corundum-bearing mineral assemblages. Lithos, 57, 143–161.
Okay, A.I. (1994) Sapphirine and Ti-clinohumite in ultra-high-pressure garnet-pyroxenite and eclogite from Dabie Shan, China. Contributions to Mineralogy and Petrology, 116, 145–155.
Podlesskii, K.K., Aranovich, L.Y., Gerya, T.V., and Kosyakova, N.A. (2008) Sapphirine-bearing assemblages in the system MgO-Al_2O_3-SiO_2: a continuing ambiguity. European Journal of Mineralogy, 20, 721–734.
Powell, R. and Holland, T.J.B. (1985) An internally consistent thermodynamic dataset with uncertainties and correlations: 3. Applications to geobarometry, worked examples and a computer program. Journal of Metamorphic Geology, 6, 173–204.
Rudnick, R.L., Gao, S., Ling, W.L., Liu, Y.S., and McDonough, W.F. (2004) Petrology and geochemistry of spinel peridotite xenoliths from Hannuoba and Qixia, North China craton. Lithos, 77, 609–637.
Santosh, M., Tsunogae, T., Li, J.H., and Liu, S.J. (2007) Discovery of sapphirine bearing Mg-Al granulites in the North China Craton: Implications for Paleoproterozoic ultrahigh temperature metamorphism. Gondwana Research, 11, 263–285.
Santosh, M., Sajeev, K., Li, J.H., Liu, S.J., and Itaya, T. (2009) Counterclockwise exhumation of a hot orogen: The Paleoproterozoic ultrahigh-temperature granulites in the North China Craton. Lithos, 110, 140–152.
Santosh, M., Liu, S.J., Tsunogae, T., and Li, J.H. (2012) Paleoproterozoic ultrahigh-temperature granulites in the North China Craton: Implications for tectonic models on extreme crustal metamorphism. Precambrian Research, in press, DOI: 10.1016/j.precamres.2011.05.003.
Sato, K., Miyamoto, T., and Kawasaki, T. (2006) Experimental calibration of sapphirine-spinel Fe^{2+}-Mg exchange thermometer: Implication for constraints on *P-T* condition of Howard Hills, Napier Complex, East Antarctica. Gondwana Research, 9, 398–408.
Seifert, F. (1974) Stability of sapphirine: a study of the aluminous part of the system MgO-Al_2O_3-SiO_2-H_2O. Journal of Geology, 82, 173–204.
Sills, J.D., Ackermand, D., Herd, R.K., and Windley, B.F. (1983) Bulk composition and mineral parageneses of sapphirine-bearing rocks along a gabbro-lherzolite contact at Finerao, Ivrea Zone, N. Italy. Journal of Metamorphic Geology, 1, 337–351.
Sobolev, A.V., Hofmann, A.W., Sobolev, S.V., and Nikogosian, I.K. (2005) An olivine-free mantle source of Hawaiian shield basalts. Nature, 434, 590–597.
Su, B.X., Zhang, H.F., Wang, Q.Y., Sun, H., Xiao, Y., and Ying, J.F. (2007) Spinel-garnet phase transition zone of Cenozoic lithospheric mantle beneath the eastern China and western Qinling and its T-P conditions. Acta Petrologica Sinica, 23, 1313–1320 (in Chinese with English abstract).
Su, B.X., Zhang, H.F., Sakyi, P.A., Yang, Y.H., Ying, J.F, Tang, Y.J., Qin, K.Z., Xiao, Y., Zhao, X.M., Mao, Q., and Ma, Y.G. (2011) The origin of spongy texture of mantle xenolith minerals from the Western Qinling, Central China. Contributions to Mineralogy and Petrology, 161, 465–482.
Sutherland, F.L., Coenraads, R.R., Schwarz, D., Raynor, L.R., Barron, B.J., and Webb, G.B. (2003) Al-rich diopside in alluvial ruby and corundum-bearing xenoliths, Australian and SE Asian basalt fields. Mineralogical Magazine, 67, 717–732.
Tang, Y.J., Zhang, H.F., Nakamura, E., Moriguti, T., Kobayashi, K., and Ying, J.F. (2007) Lithium isotopic systematics of peridotite xenoliths from Hannuoba, North China Craton: implications for melt-rock interaction in the considerably thinned lithospheric mantle. Geochimica et Cosmochimica Acta, 71, 4327–4341.
Tang, Y.J., Zhang, H.F., Nakamura, E., and Ying, J.F. (2011) Multistage melt/fluid-peridotite interactions in the refertilized lithospheric mantle beneath the North China Craton: constraints from the Li-Sr-Nd isotopic disequilibrium between minerals of peridotite xenoliths. Contributions to Mineralogy and Petrology, 161, 845–861.
Tsunogae, T. and Santosh, M. (2011) Sapphirine + quartz assemblage from the Southern Granulite Terrane, India: diagnostic evidence for ultrahigh-temperature metamorphism within the Gondwana collisional orogen. Geological Journal, 46, 183–197.
Tsunogae, T., Liu, S.J., Santosh, M., Shimizu, H., and Li, J.H. (2011) Ultrahigh-temperature metamorphism in Daqingshan, Inner Mongolia Suture Zone, North China Craton. Gondwana Research, 20, 36–47.
Xiang, H., Zhang, L., Zhong, Z.Q., Santosh, M., Zhou, H.W., Zhang, H.F., Zheng, J.P., and Zheng, S. (2012) Ultrahigh-temperature metamorphism and anticlockwise *P-T*-t path of Paleozoic granulites from north Qingling-Tongbai orogen, Central China. Gondwana Research, 21, 559–576, DOI: 10.1016/j.gr.2011.07.002.
Xu, Y.G. (2002) Evidence for crustal components in the mantle and constraints on the crustal recycling mechanisms: pyroxenite xenoliths from Hannuoba, North China. Chemical Geology, 182, 301–322.
Yu, S.Y., Xu, Y.G., Ma, J.L., Zheng, Y.F., Kuang, Y.S., Hong, L.B., Ge, W.C., and Tong, L.X. (2010) Remnants of oceanic lower crust in the subcontinental lithospheric mantle: trace element and Sr-Nd-O isotope evidence from aluminous garnet pyroxenite xenoliths from Jiaohe, Northeast China. Earth and Planetary Science Letters, 297, 413–422.
Zhang, H.F. (2009) Peridotite-melt interaction: a key point for the destruction of cratonic lithospheric mantle. Chinese Science Bulletin, 54, 3417–3437.
Zhang, H.F., Nakamura, E., Kobayashi, K., Ying, J.F., and Tang, Y.J. (2010) Recycled crustal melt injection into lithospheric mantle: implication from cumulative composite and pyroxenite xenoliths. International Journal of Earth Sciences, 99, 1167–1186.
Zhang, H.F., Ying, J.F., Tang, Y.J., Li, X.H., Feng, C., and Santosh, M. (2011) Phanerozoic reactivation of the Archean North China Craton through episodic magmatism: Evidence from zircon U-Pb geochronology and Hf isotopes from the Liaodong Peninsula. Gondwana Research, 19, 446–459.
Zhang, H.F., Zhu, R.X., Santosh, M., Ying, J.F., Su, B.X., and Hu, Y. (2012) Episodic widespread magma underplating beneath the North China Craton in the Phanerozoic: Implications for craton destruction. Gondwana Research, in press, DOI: 10.1016/j.gr.2011.12.006.
Zheng, J.P., Griffin, W.L., Qi, L., O'Reilly, S.Y., Sun, M., Zheng, S., Pearson, N., Gao, J.F., Yu, C.M., Su, Y.P., Tang, H.Y., Liu, Q.S., and Wu, X.L. (2009) Age and composition of granulite and pyroxenite xenoliths in Hannuoba basalts reflect Paleogene underplating beneath the North China Craton. Chemical Geology, 264, 266–280.
Zhou, X.H., Sun, M., Zhang, G.H., and Chen, S.H. (2002) Continental crust and lithospheric mantle interaction beneath North China: isotopic evidence from granulite xenoliths in Hannuoba, Sino-Korean craton. Lithos, 62, 111–124.

Manuscript received April 12, 2011
Manuscript accepted February 4, 2012
Manuscript handled by Matthias Gottschalk